

Supporting Information

This document contains the following:

1. A section on details on the CTR-models with tables containing the coordinates of atoms for the surface models for the fresh (Table SI1) and aged (Table SI2) samples plus a the surface model for the unrelaxed bulk termination of hematite (Table SI3)
2. A section on details on the surface complexation models for the fresh and aged hematite samples.

CTR-model details

Table S11: Fractional coordinates of atoms in the adjusted surface model for the fresh hematite sample. Additional to the fractional coordinates, z displacement (Δz), Debye-Waller Parameter (U_{iso}), Occupancy (Occ), and Bond Valence Sum (BVS) are reported. ($\chi^2 = 3.97$, $n = 524$, $p = 41$, roughness(β) = 0.17(1))

| Layer | Relaxed surface model | | | | | | |
|--|-----------------------|----------|----------|----------------|-----------------------------|---------|------|
| | x | y | z | Δz (Å) | U_{iso} (Å ²) | Occ. | BVS |
| Domain 1: O ₃ -Fe-Fe-R termination (44.4(1) %) | | | | | | | |
| 1 O | 0.361(1) | 0.00(8) | 1.00(3) | -0.1(4) | 0.03(3) | 0.76(2) | - |
| | 0.64(8) | 0.640(1) | 1.00(3) | -0.1(4) | 0.03(3) | 0.76(2) | - |
| | 0.99(8) | 0.36(8) | 1.00(3) | -0.1(4) | 0.03(3) | 0.76(2) | - |
| 2 Fe | 0.0000 | 0.0000 | 0.928(1) | -0.15(1) | 0.022(4) | 1 | 3.01 |
| 3 Fe | 0.3333 | 0.6667 | 0.913(1) | 0.25(2) | 0.028(1) | 1 | 2.98 |
| 4 O | 0.99(5) | 0.693(1) | 0.83(9) | 0 (1) | 0.03(1) | 1 | - |
| | 0.70(5) | 0.00(5) | 0.83(9) | 0 (1) | 0.03(1) | 1 | - |
| | 0.31(5) | 0.30(5) | 0.83(9) | 0 (1) | 0.03(1) | 1 | - |
| 5 Fe | 0.6667 | 0.3333 | 0.77(8) | 0 (1) | 0.012 | 1 | 2.99 |
| 6 Fe | 0.0000 | 0.0000 | 0.738(7) | 0.14 (9) | 0.012 | 1 | 2.99 |
| 7 O | 0.9726 | 0.3333 | 0.665* | 0 (9) | 0.015 | 1 | - |
| | 0.6667 | 0.6392 | 0.665* | 0 (9) | 0.015 | 1 | - |
| | 0.3608 | 0.0274 | 0.665* | 0 (9) | 0.015 | 1 | - |
| 8 Fe | 0.3333 | 0.6667 | 0.6053 | 0 | 0.012 | 1 | 3.02 |
| 9 Fe | 0.6667 | 0.3333 | 0.5614 | 0 | 0.012 | 1 | 3.02 |
| 10 O | 0.0274 | 0.6667 | 0.5000 | 0 | 0.015 | 1 | - |
| | 0.3333 | 0.3608 | 0.5000 | 0 | 0.015 | 1 | - |
| | 0.6392 | 0.9726 | 0.5000 | 0 | 0.015 | 1 | - |
| Domain 2: O ₃ -Fe-O ₃ -R termination (55.6(1) %) | | | | | | | |
| 1 O | 0.329(1) | 0.958(7) | 1.02(1) | 0.3(1) | 0.04(1) | 0.73(1) | - |
| | 0.629(8) | 0.671(1) | 1.02(1) | 0.3(1) | 0.04(1) | 0.73(1) | - |
| | 0.041(8) | 0.371(8) | 1.02(1) | 0.3(1) | 0.04(1) | 0.73(1) | - |
| 2 Fe | - | - | - | - | - | 0 | - |
| 3 Fe | 0.3333 | 0.6667 | 0.891(3) | -0.04(5) | 0.013(6) | 1 | 2.97 |
| 4 O | 0.028(5) | 0.690(1) | 0.822(4) | -0.16(6) | 0.04(1) | 1 | - |
| | 0.663(6) | 0.973(5) | 0.822(4) | -0.16(6) | 0.04(1) | 1 | - |
| | 0.310(6) | 0.337(6) | 0.822(4) | -0.16(6) | 0.04(1) | 1 | - |
| 5 Fe | 0.6667 | 0.3333 | 0.77(8) | 0(1) | 0.012 | 1 | 3.02 |
| 6 Fe | 0.0000 | 0.0000 | 0.73(1) | 0.1(1) | 0.012 | 1 | 3.05 |
| 7 O | 0.9726 | 0.3333 | 0.666* | 0 (9) | 0.015 | 1 | - |
| | 0.6667 | 0.6392 | 0.666* | 0 (9) | 0.015 | 1 | - |
| | 0.3608 | 0.0274 | 0.666* | 0 (9) | 0.015 | 1 | - |
| 8 Fe | 0.3333 | 0.6667 | 0.606(8) | 0.0(1) | 0.012 | 1 | 3.03 |
| 9 Fe | 0.6667 | 0.3333 | 0.564(2) | 0.03(3) | 0.012 | 1 | 3.04 |
| 10 O | 0.0274 | 0.6667 | 0.50(1) | 0.0(2) | 0.015 | 1 | - |
| | 0.3333 | 0.3608 | 0.50(1) | 0.0(2) | 0.015 | 1 | - |
| | 0.6392 | 0.9726 | 0.50(1) | 0.0(2) | 0.015 | 1 | - |

Uncertainties are reported at the 2 σ level. They are given in parenthesis for the last significant digit.

Parameters without a reported uncertainty were not adjusted during structure refinement. *: the z-Parameters of the layers marked with an asterisk are highly correlated with other parameters and have therefore very high uncertainties, which are not reported in the fractional coordinates, but only in the Δz column.

Table S12: Fractional coordinates of atoms in the adjusted surface model for the aged hematite sample. Additional to the fractional coordinates, z displacement (Δz), Debye-Waller Parameters (U_{iso}), Occupancy (Occ), and Bond Valence Sum (BVS) are reported. ($\chi^2 = 2.97$, $n = 439$, $p = 43$, roughness(β) = 0.18(1))

| Layer | Relaxed surface model | | | | | | |
|--|-----------------------|----------|----------|----------------|-----------------------------|---------|------|
| | x | y | z | Δz (Å) | U_{iso} (Å ²) | Occ. | BVS |
| Domain 1: O ₃ -Fe-Fe-R termination (67.8(1) %) | | | | | | | |
| 1 O | 0.340(1) | 0.978(4) | 0.996(7) | -0.1(1) | 0.050(7) | 1 | - |
| | 0.637(5) | 0.660(1) | 0.996(7) | -0.1(1) | 0.050(7) | 1 | - |
| | 0.023(5) | 0.363(5) | 0.996(7) | -0.1(1) | 0.050(7) | 1 | - |
| 2 Fe | 0.0000 | 0.0000 | 0.925(1) | -0.184(6) | 0.060(1) | 1 | 3.04 |
| 3 Fe | 0.3333 | 0.6667 | 0.894(1) | 0.0(1) | 0.034(1) | 1 | 3.05 |
| 4 O | 0.000(3) | 0.694(1) | 0.83(6) | 0.0(8) | 0.03(1) | 1 | - |
| | 0.694(3) | 0.000(3) | 0.83(6) | 0.0(8) | 0.03(1) | 1 | - |
| | 0.306(3) | 0.306(3) | 0.83(6) | 0.0(8) | 0.03(1) | 1 | - |
| 5 Fe | 0.6667 | 0.3333 | 0.77(1) | 0.0(2) | 0.012 | 1 | 3.01 |
| 6 Fe | 0.0000 | 0.0000 | 0.734(6) | 0.09(9) | 0.012 | 1 | 3.03 |
| 7 O | 0.9726 | 0.3333 | 0.67(5) | 0.0(7) | 0.015 | 1 | - |
| | 0.6667 | 0.6392 | 0.67(5) | 0.0(7) | 0.015 | 1 | - |
| | 0.3608 | 0.0274 | 0.67(5) | 0.0(7) | 0.015 | 1 | - |
| 8 Fe | 0.3333 | 0.6667 | 0.6053 | 0 | 0.012 | 1 | 2.94 |
| 9 Fe | 0.6667 | 0.3333 | 0.5614 | 0 | 0.012 | 1 | 2.94 |
| 10 O | 0.0274 | 0.6667 | 0.5000 | 0 | 0.015 | 1 | - |
| | 0.3333 | 0.3608 | 0.5000 | 0 | 0.015 | 1 | - |
| | 0.6392 | 0.9726 | 0.5000 | 0 | 0.015 | 1 | - |
| Domain 2: O ₃ -Fe-O ₃ -R termination (32.2(1) %) | | | | | | | |
| 0 O (H ₂ O) | 0.085(3) | 0.385(1) | 1.16(7) | - | 0.06(1) | 0.57(1) | - |
| | 0.300(3) | 0.915(3) | 1.16(7) | - | 0.06(1) | 0.57(1) | - |
| | 0.615(3) | 0.700(3) | 1.16(7) | - | 0.06(1) | 0.57(1) | - |
| 1 O | 0.302(1) | 0.0(4) | 1.00(3) | 0.0(4) | 0.10(1) | 1 | - |
| | 0.7(4) | 0.698(1) | 1.00(3) | 0.0(4) | 0.10(1) | 1 | - |
| | 0.0(4) | 0.3(4) | 1.00(3) | 0.0(4) | 0.10(1) | 1 | - |
| 2 Fe | - | - | - | - | - | 0 | - |
| 3 Fe | 0.3333 | 0.6667 | 0.931(1) | 0.50(1) | 0.056(2) | 1 | 2.97 |
| 4 O | 0.035(4) | 0.693(1) | 0.83(7) | 0(1) | 0.04(1) | 1 | - |
| | 0.658(1) | 0.964(4) | 0.83(7) | 0(1) | 0.04(1) | 1 | - |
| | 0.307(4) | 0.343(4) | 0.83(7) | 0(1) | 0.04(1) | 1 | - |
| 5 Fe | 0.6667 | 0.3333 | 0.757(1) | -0.21(2) | 0.012 | 1 | 3.03 |
| 6 Fe | 0.0000 | 0.0000 | 0.73(4) | 0.0(6) | 0.012 | 1 | 2.89 |
| 7 O | 0.9726 | 0.3333 | 0.67(2) | 0.1(2) | 0.015 | 1 | - |
| | 0.6667 | 0.6392 | 0.67(2) | 0.1(2) | 0.015 | 1 | - |
| | 0.3608 | 0.0274 | 0.67(2) | 0.1(2) | 0.015 | 1 | - |
| 8 Fe | 0.3333 | 0.6667 | 0.607(5) | 0.03(7) | 0.012 | 1 | 2.90 |
| 9 Fe | 0.6667 | 0.3333 | 0.561* | 0(3) | 0.012 | 1 | 2.91 |
| 10 O | 0.0274 | 0.6667 | 0.504(6) | 0.05(9) | 0.015 | 1 | - |
| | 0.3333 | 0.3608 | 0.504(6) | 0.05(9) | 0.015 | 1 | - |
| | 0.6392 | 0.9726 | 0.504(6) | 0.05(9) | 0.015 | 1 | - |

Uncertainties are reported at the 2 σ level. They are given in parenthesis for the last significant digit. Parameters without a reported uncertainty were not adjusted during structure refinement. *: the z-Parameters marked with an asterisk are highly correlated with other parameters and have therefore very high uncertainties, which are not reported in the fractional coordinates, but only in the Δz column.

Structural coordinates of the bulk terminated hematite structure are reported in Table S13.

Tabelle S13: Fractional coordinates and Debye-Waller Parameters (U_{iso}) of atoms in the surface model for the unrelaxed bulk termination of hematite.

| Layer | Bulk termination | | | |
|-------|------------------|--------|--------|---------------------------------|
| | x | y | z | $U_{\text{iso}} (\text{\AA}^2)$ |
| 1 O | 0.3333 | 0.9726 | 1.0000 | 0.015 |
| | 0.6392 | 0.6667 | 1.0000 | 0.015 |
| | 0.0274 | 0.3608 | 1.0000 | 0.015 |
| 2 Fe | 0 | 0 | 0.9386 | 0.012 |
| 3 Fe | 0.3333 | 0.6667 | 0.8947 | 0.012 |
| 4 O | 0.0000 | 0.6941 | 0.8333 | 0.015 |
| | 0.3059 | 0.3059 | 0.8333 | 0.015 |
| | 0.6941 | 0.0000 | 0.8333 | 0.015 |
| 5 Fe | 0.6667 | 0.3333 | 0.7720 | 0.012 |
| 6 Fe | 0.0000 | 0.0000 | 0.7280 | 0.012 |
| 7 O | 0.9726 | 0.3333 | 0.6667 | 0.015 |
| | 0.6667 | 0.6392 | 0.6667 | 0.015 |
| | 0.3608 | 0.0274 | 0.6667 | 0.015 |
| 8 Fe | 0.3333 | 0.6667 | 0.6053 | 0.012 |
| 9 Fe | 0.6667 | 0.3333 | 0.5614 | 0.012 |
| 10 O | 0.0274 | 0.6667 | 0.5000 | 0.015 |
| | 0.3333 | 0.3608 | 0.5000 | 0.015 |
| | 0.6392 | 0.9726 | 0.5000 | 0.015 |

Surface complexation model details

The models for the two samples are given in some details. As indicated in the text the slip plane distance is the major parameter for well describing the numerical values of the zeta-potentials. The slip plane distance has been used as in previous work¹⁻³. We define an empirical slip plane distance (s) as the distance between the onset of the diffuse layer and the location of the electrokinetic plane; the value of s was considered to be ionic strength dependent as suggested for mineral surfaces by others^{1,2}. As previously observed, initial calculations with $s = 0$ nm yielded too high zeta potentials; tests with $s = \text{const.}$ (*i.e.* independent of ionic strength) could not reproduce the ionic strength dependence of the zeta potentials; the slip plane distance was therefore related to the Debye-length (*i.e.* $s = x/\kappa$, where $1/\kappa$ is the ionic strength dependent Debye length) and only the parameter x remains to be determined for a given system. If $x = 1$, the slip plane is found at the Debye-length.

Fresh hematite surface

Figure SI1 shows the conceptual model implemented for the surface complexation calculations and Table SI4 summarizes the model for the fresh surface and the model parameters.

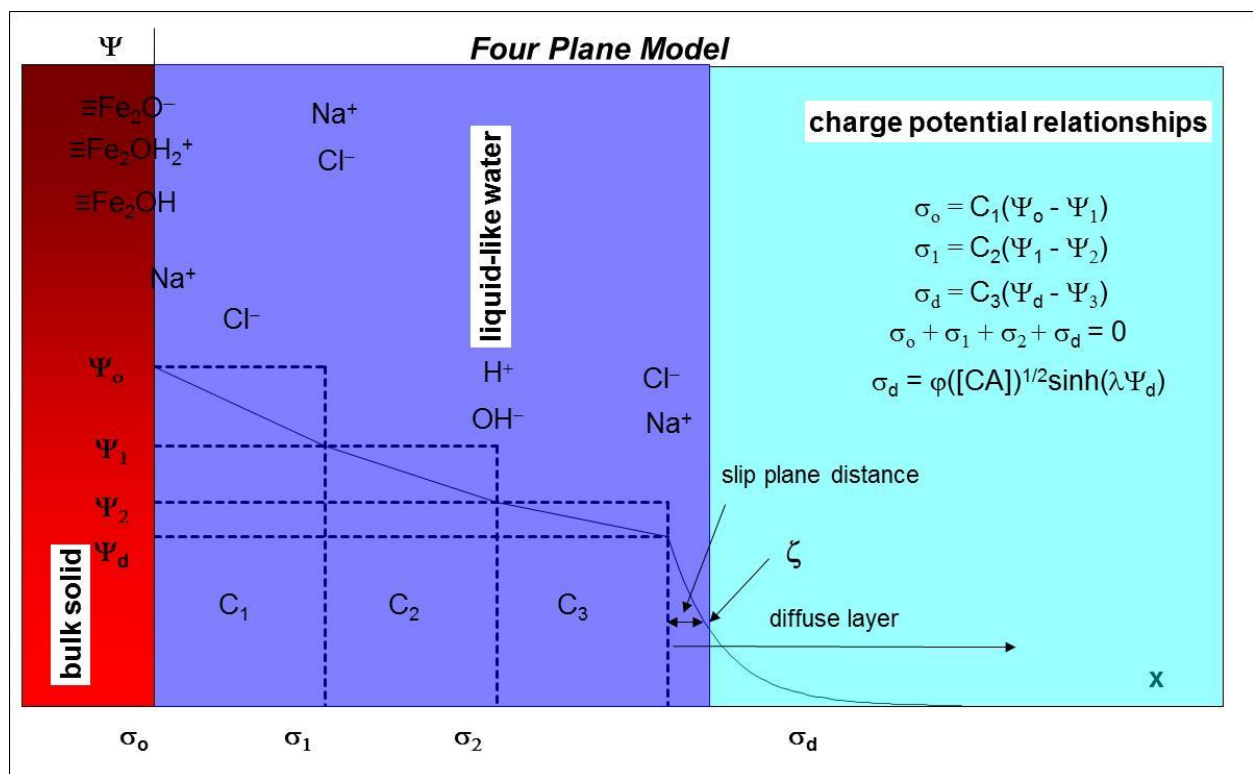


Figure SI1. Schematic sketch of the surface complexation model applied for the fresh hematite surface.

The reaction equations involve two sites, the surface hydroxyls ($\equiv\text{Fe}_2\text{OH}$) and a water site ($\equiv\text{H}_2\text{O}$) with fixed site densities. The water site model is identical to the one used previously for many inert surfaces³. The stability constants were optimized except for those marked with an asterisk, which were fixed at common values. The charge transfer factors indicate to which plane the adsorbing charge was attributed. Only the adsorption of the chloride ion to the neutral surface hydroxyl involved charge distribution. The adsorption of sodium and chloride ions to the neutral hydroxyl

groups are based on the independent observations mentioned in the main text, that suggest the formation of CaCl_2 rows (gibbsite basal planes⁴) or salt hydrates (hematite basal planes⁵). The interaction as modelled here involves the occupation of 3 hydroxyl sites (b-coefficient). In the mass law equation (a-coefficient) a value of 1 is used. This issue has been at length discussed elsewhere⁶ and the present treatment avoids variation of the log K value with solid to liquid ratio. The value of 3 was applied to the mole balance assuming that the adsorption occurs in the hexameric rings of the ideal structure, such that three surface groups are consumed for each entity adsorbed.

The log K values for protonation and deprotonation of the neutral surface groups concur with previous estimates⁷⁻⁹.

The model for the second site ($\equiv\text{H}_2\text{O}$) is similar to the one previously used³, except that it is shifted further away from the surface. The estimated Log K values compare extremely well to previous results^{3,10}.

Only the capacitance C_1 was optimized, while C_2 and C_3 were adopted from the previous water layer model³. The slip plane separation, s , is quite low, which means that the model inherent slip plane is relatively far out in the diffuse layer. A value of $s = 0$ nm ($x = 0$) would mean it coincides with the head end of the diffuse layer.

Table SI4. Chemical equilibrium reactions, stability constants at infinite dilution, charge transfer and deviations from traditional stoichiometric coefficients for the thermodynamic model used to describe fresh hematite.

| Reaction equation | log K | charge transfer | Stoichiometry deviations |
|--|--------|--|--|
| $\equiv\text{Fe}_2\text{OH} + \text{H}^+ \leftrightarrow \equiv\text{Fe}_2\text{OH}_2^+$ | 3.17 | $\Delta z_0 = +1$ | |
| $\equiv\text{Fe}_2\text{OH}_2^+ + \text{Cl}^- \leftrightarrow \equiv\text{Fe}_2\text{OH}_2^+\text{Cl}^-$ | -0.80* | $\Delta z_1 = -1$ | |
| $\equiv\text{Fe}_2\text{OH} \leftrightarrow \equiv\text{Fe}_2\text{O}^- + \text{H}^+$ | -11.60 | $\Delta z_0 = -1$ | |
| $\equiv\text{Fe}_2\text{O}^- + \text{Na}^+ \leftrightarrow \equiv\text{Fe}_2\text{O}^-\text{Na}^+$ | -0.80* | $\Delta z_1 = 1$ | |
| $\equiv\text{Fe}_2\text{OH} + \text{Na}^+ \leftrightarrow \equiv\text{Fe}_2\text{OHNa}^+$ | 3.11 | $\Delta z_0 = 1$ | $a(\equiv\text{Fe}_2\text{OH}) = 1, b(\equiv\text{Fe}_2\text{OH}) = 3$ |
| $\equiv\text{Fe}_2\text{OH} + \text{Cl}^- \leftrightarrow \equiv\text{Fe}_2\text{OHCl}^-$ | 2.55 | $\Delta z_0 = -0.5, \Delta z_1 = -0.5$ | $a(\equiv\text{Fe}_2\text{OH}) = 1, b(\equiv\text{Fe}_2\text{OH}) = 3$ |
| $\equiv\text{H}_2\text{O} + \text{H}^+ \leftrightarrow \equiv\text{H}_2\text{OH}^+$ | 1.14 | $\Delta z_2 = 1$ | |
| $\equiv\text{H}_2\text{OH}^+ + \text{Cl}^- \leftrightarrow \equiv\text{H}_2\text{OH}^+\text{Cl}^-$ | -0.50* | $\Delta z_3 = -1$ | |
| $\equiv\text{H}_2\text{O} \leftrightarrow \equiv\text{HO}^- + \text{H}^+$ | -6.61 | $\Delta z_2 = -1$ | |
| $\equiv\text{HO}^- + \text{Na}^+ \leftrightarrow \equiv\text{HO}^-\text{Na}^+$ | 0.13 | $\Delta z_3 = 1$ | |

Site densities are 13.7 ($\equiv\text{Fe}_2\text{OH}$) and 17.3 ($\equiv\text{H}_2\text{O}$) sites/nm², respectively. Capacitance values are 3.5 F/m² (C_1), 0.20 F/m² (C_2) and 0.21 F/m² (C_3).

Slip plane distance parameter: $x = 0.25$.

Aged hematite surface

Figure S12 shows the conceptual model implemented for the surface complexation calculations and Table S15 summarizes the model for the aged surface and the model parameters.

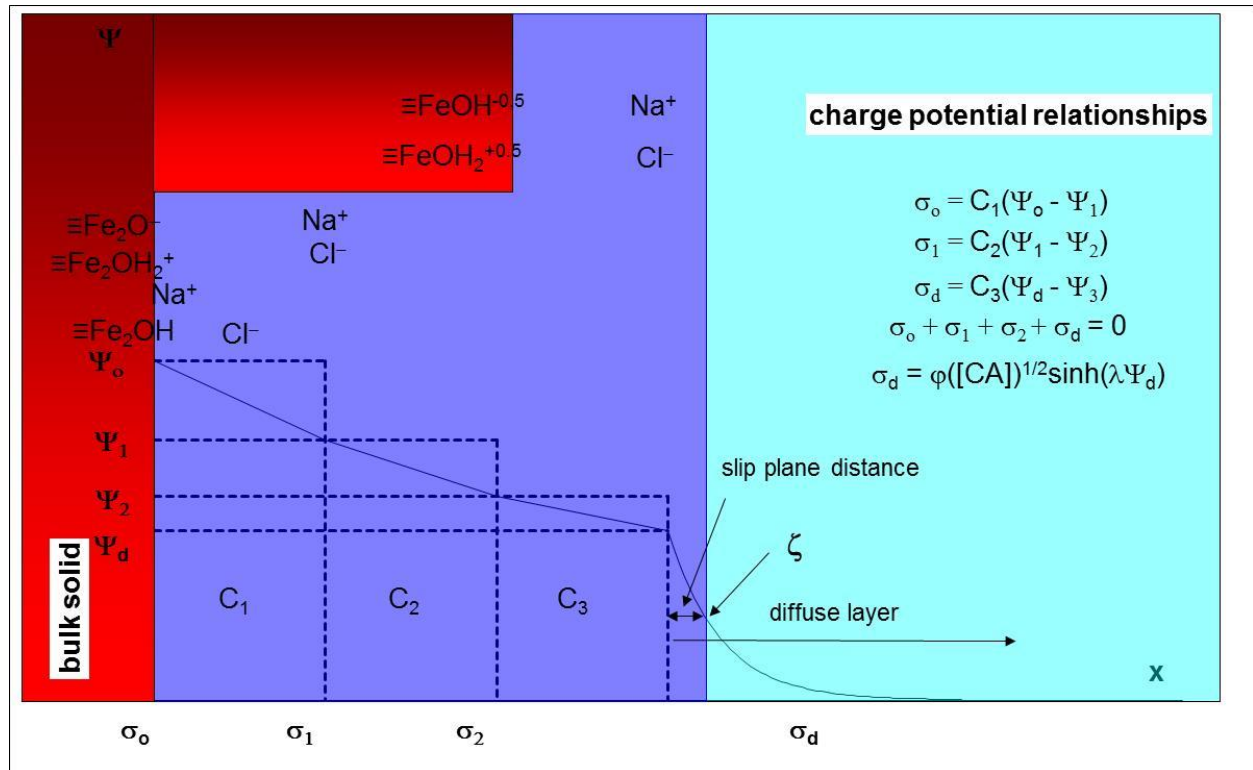


Figure S12. Schematic sketch of the surface complexation model applied for the aged hematite surface.

The reaction equations involve two sites, the doubly coordinated surface hydroxyls ($\equiv\text{Fe}_2\text{OH}$) and the singly coordinated surface hydroxyls ($\equiv\text{FeOH}$) with the specified site densities, which were inferred from the CTR-data. We assume that the singly coordinated hydroxyls are active in the present case, since water appears to strongly interact with the surface (as shown in the CTR study). The singly coordinated surface hydroxyls ($\equiv\text{FeOH}$) are placed away from the surface plane (i.e. the plane where the doubly coordinated groups reside). The stability constants were optimized except for those marked with an asterisk, which were fixed at common values. The log K values for protonation and deprotonation of the doubly-coordinated surface groups were taken from the previous estimates for the fresh sample. It turned out that the sodium and chloride association constants to the doubly-coordinated surface groups became lower, which might be taken as a further indication for interference from the singly coordinated groups.

The model for the second site ($\equiv\text{FeOH}$) is similar to one previously used¹¹, except that the charge of this group is put into the 2-plane, i.e. away from the doubly coordinated groups. Log K values are comparable as well¹¹.

All the capacitances were optimized in this case. They were found to be in the range typically found for oxide-electrolyte interfaces¹². The slip plane separation parameter is higher, which places the slip plane further away from the onset of the diffuse layer than in the case of the fresh hematite. Only one salt concentration was available in the case of the aged hematite and the slip plane parameter

was adjusted to that curve only, while in the case of the fresh hematite it was fitted to three salt contents simultaneously as discussed in the main text.

Table SI5. Chemical equilibrium reactions, stability constants at infinite dilution, charge transfer and deviations from traditional stoichiometric coefficients for the thermodynamic model used in the main text.

| Reaction equation | log K | charge transfer | Stoichiometry deviations |
|---|--------|--|--|
| $\equiv\text{Fe}_2\text{OH} + \text{H}^+ \leftrightarrow \equiv\text{Fe}_2\text{OH}_2^+$ | 3.17 | $\Delta z_0 = +1$ | |
| $\equiv\text{Fe}_2\text{OH}_2^+ + \text{Cl}^- \leftrightarrow \equiv\text{Fe}_2\text{OH}_2^{+\dots}\text{Cl}^-$ | -0.80* | $\Delta z_1 = -1$ | |
| $\equiv\text{Fe}_2\text{OH} \leftrightarrow \equiv\text{Fe}_2\text{O}^- + \text{H}^+$ | -11.60 | $\Delta z_0 = -1$ | |
| $\equiv\text{Fe}_2\text{O}^- + \text{Na}^+ \leftrightarrow \equiv\text{Fe}_2\text{O}^{-\dots}\text{Na}^+$ | -0.80* | $\Delta z_1 = 1$ | |
| $\equiv\text{Fe}_2\text{OH} + \text{Na}^+ \leftrightarrow \equiv\text{Fe}_2\text{OHNa}^+$ | 1.94 | $\Delta z_0 = 1$ | $a(\equiv\text{Fe}_2\text{OH}) = 1, b(\equiv\text{Fe}_2\text{OH}) = 3$ |
| $\equiv\text{Fe}_2\text{OH} + \text{Cl}^- \leftrightarrow \equiv\text{Fe}_2\text{OHCl}^-$ | 2.18 | $\Delta z_0 = -0.5, \Delta z_1 = -0.5$ | $a(\equiv\text{Fe}_2\text{OH}) = 1, b(\equiv\text{Fe}_2\text{OH}) = 3$ |
| $\equiv\text{FeOH}^{-0.5} + \text{H}^+ \leftrightarrow \equiv\text{FeOH}_2^{+0.5}$ | 8.88 | $\Delta z_2 = +1$ | |
| $\equiv\text{FeOH}_2^{+0.5} + \text{Cl}^- \leftrightarrow \equiv\text{FeOH}_2^{+0.5\dots}\text{Cl}^-$ | -0.80* | $\Delta z_3 = -1$ | |
| $\equiv\text{FeOH}^{-0.5} + \text{Na}^+ \leftrightarrow \equiv\text{FeOH}^{-0.5\dots}\text{Na}^+$ | -0.80* | $\Delta z_3 = -1$ | |

Site densities are 9.3 ($\equiv\text{Fe}_2\text{OH}$) and 4.4 ($\equiv\text{FeOH}^{-0.5}$).

Capacitance values are 1.12 F/m² (C₁), 1.16 F/m² (C₂) and 1.22 F/m² (C₃).

Slip plane distance parameter: $x = 0.70$.

References

1. K. Bourikas, T. Hiemstra and W. H. Van Riemsdijk, *Langmuir*, 2001, **17**, 749-756.
2. H. Yong and W. H. Van Riemsdijk, *Langmuir*, 1999, **15**, 5942-5955.
3. J. Luetzenkirchen, T. Preocanin and N. Kallay, *Physical Chemistry Chemical Physics*, 2008, **10**, 4946-4955.
4. I. Siretanu, D. Ebeling, M. P. Andersson, S. L. S. Stipp, A. Philipse, M. C. Stuart, D. van den Ende and F. Mugele, *Scientific Reports*, 2014, **4**.
5. A. Shchukarev, J.-F. Boily and A. R. Felmy, *Journal of Physical Chemistry C*, 2007, **111**, 18307-18316.
6. J. Lützenkirchen, R. Marsac, D. A. Kulik, T. E. Payne, Z. Xue, S. Orsetti and S. B. Haderlein, *Applied Geochemistry*.
7. D. Yang, M. Krasowska, R. Sedev and J. Ralston, *Physical Chemistry Chemical Physics*, 2010, **12**, 13724-13729.
8. T. Hiemstra and W. H. Van Riemsdijk, *Langmuir*, 1999, **15**, 8045-8051.
9. L. Zhang, C. Tian, G. A. Waychunas and Y. R. Shen, *J. Am. Chem. Soc.*, 2008, **130**, 7686-7694.
10. J. Lutzenkirchen, C. Richter and F. Brandenstein, *Adsorpt.-J. Int. Adsorpt. Soc.*, 2010, **16**, 249-258.
11. J. Luetzenkirchen, T. Preocanin, F. Stipic, F. Heberling, J. Rosenqvist and N. Kallay, *Geochim. Cosmochim. Acta*, 2013, **120**, 479-486.
12. T. Hiemstra and W. H. Van Riemsdijk, *Colloids and Surfaces*, 1991, **59**, 7-25.